Current driven domain wall dynamics in ferrimagnetic strips explained by means of a two interacting sublattices model

Eduardo Martínez (iD), Víctor Raposo (iD), and Óscar Alejos (iD)
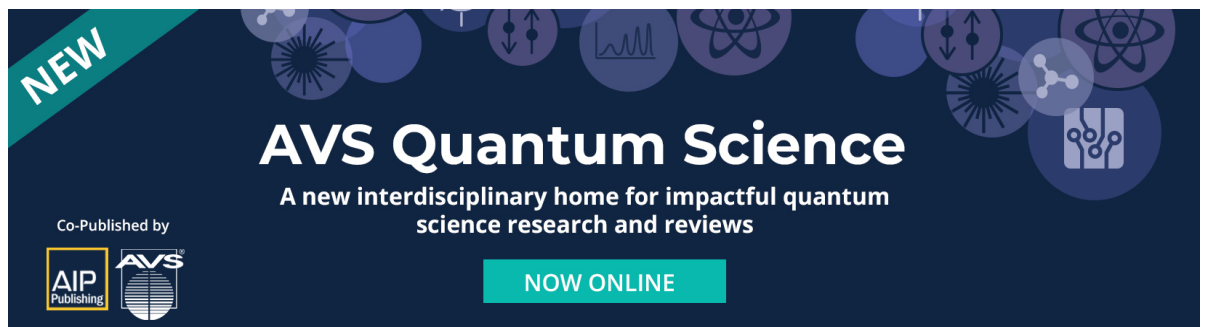
View Online   Export Citation   CrossMark

ARTICLES YOU MAY BE INTERESTED IN

Perspective: Magnetic skyrmions−Overview of recent progress in an active research field
Journal of Applied Physics **124**, 240901 (2018); https://doi.org/10.1063/1.5048972

Multilayered current-induced domain wall motion in Pt/Tb-Co/Ta/Tb-Co/Pt magnetic wire
AIP Advances **8**, 025309 (2018); https://doi.org/10.1063/1.5017814

Correlation between magnetic properties and depinning field in field-driven domain wall dynamics in GdFeCo ferrimagnets
Applied Physics Letters **112**, 172403 (2018); https://doi.org/10.1063/1.5022809

Current driven domain wall dynamics in ferrimagnetic strips explained by means of a two interacting sublattices model

View Online   Export Citation   CrossMark

Eduardo Martínez,[1] [iD] Víctor Raposo,[1] [iD] and Óscar Alejos[2,a] [iD]

AFFILIATIONS

[1] Dpto. Física Aplicada, Universidad de Salamanca, 37008 Salamanca, Spain
[2] Dpto. Electricidad y Electrónica, Universidad de Valladolid, 47011 Valladolid, Spain

Note: This paper was presented at the 64th Annual Conference on Magnetism and Magnetic Materials.
[a] **Electronic mail:** oscar.alejos@uva.es.

ABSTRACT

The current-driven domain wall dynamics along ferrimagnetic elements are here theoretically analyzed as a function of temperature by means of micromagnetic simulations and a one dimensional model. Contrarily to conventional effective approaches, our model takes into account the two coupled ferromagnetic sublattices forming the ferrimagnetic element. Although the model is suitable for elements with asymmetric exchange interaction and spin-orbit coupling effects due to adjacent heavy metal layers, we here focus our attention on the case of single-layer ferrimagnetic strips where domain walls adopt achiral Bloch configurations at rest. Such domain walls can be driven by either out-of-plane fields or spin transfer torques upon bulk current injection. Our results indicate that the domain wall velocity is optimized at the angular compensation temperature for both field-driven and current-driven cases. Our advanced models allow us to infer that the precession of the internal domain wall moments is suppressed at such compensation temperature, and they will be useful to interpret state-of-the art experiments on these elements.

I. INTRODUCTION

A great effort is being devoted to the finding of optimal systems permitting fast displacement of domain walls (DWs) along racetrack elements.[1] As recent experiments demonstrate, DW velocities in the order of $1\frac{\text{km}}{\text{s}}$ can be achieved along ferrimagnetic (FiM) strips,[2,3] with a linear relationship between DW velocities and the magnitude of applied stimuli.[2–4]

Here we provide a theoretical description of DW dynamics in FiM strips based on an extended collective coordinates model (1DM).[5,6] Differently from other approaches,[7,8] based on effective parameters, our model considers such elements as formed by two ferromagnetic sublattices, and coupled by means of an interlattice exchange interaction. Full micromagnetic (μM) simulations have been performed also to back up those drawn by the 1DM. Importantly, our approaches allow to infer results not achievable from effective models, and to provide insights and interesting

predictions of the current-driven dynamics of DWs along FiM films.

Fig. 1(a) schematizes the local orientation of magnetic moments in the ferrimagnet. $\vec{m}_i(i = 1, 2)$ represent the orientations of the respective magnetic moments of each ferromagnetic sublattice. The magnetization of each sublattice is temperature dependent, so that magnetization of each sublattice vanishes at Curie temperature (T_C), with a magnetization compensation temperature T_M, as it is shown in Fig. 1(b). The temperature dependence can be described by the analytical functions: $M_{s,i}(T) = M_{s,i}^0 \left(1 - \frac{T}{T_C}\right)^{a_i}$, $M_{s,i}^0$ being the respective magnetizations at zero temperature, and a_i being dependent on the sublattice components.

The model can be applied to two different architectures. As a first architecture (Fig. 1(c)), a FiM strip on top of a heavy metal (HM) can be considered. The FiM/HM interface promotes interfacial asymmetric exchange, resulting in Néel type DWs and cur-
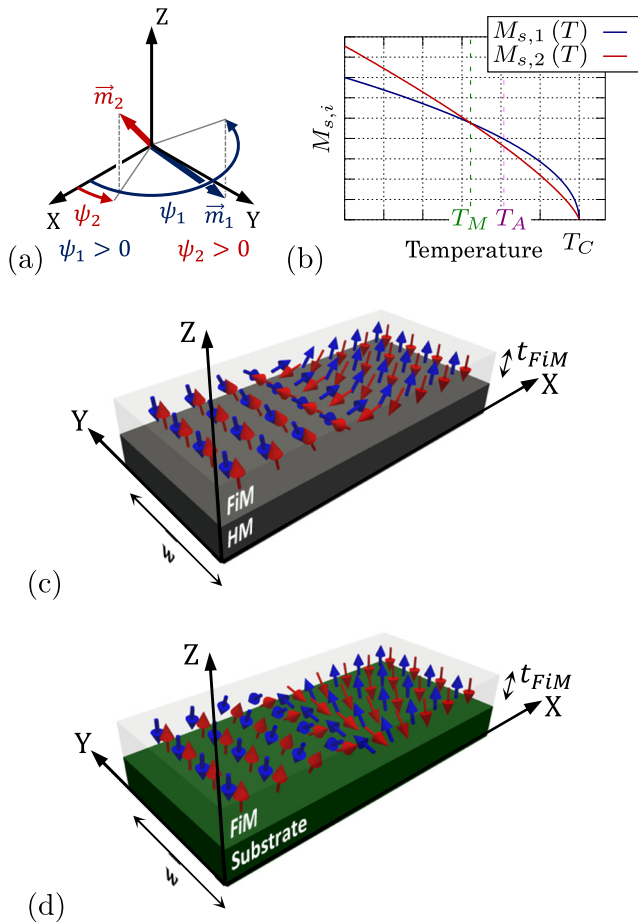
FIG. 1. Two sublattices constitute the FiM: (a) magnetizations are represented by the unit vectors $\vec{m}_1$ and $\vec{m}_2$, with in-plane orientation angles ψ_1 and ψ_2, respectively, (b) temperature dependence of the magnetization of each sublattice, (c) magnetic DW of Néel type, and (d) magnetic DW of Bloch type amidst two domains oriented out of plane (the strip width w is here shown).

rent driven domain wall motion (CDDWM) due to spin orbit torques (SOT), with rigid DWs. At the angular momentum compensation temperature (T_A), differing from T_M due to the distinct Landé factors g_i for each sublattice, DW magnetic moments keep aligned with the current, leading to a linear increase of DW velocities. Thus, DW velocities are maximized at T_A. This first architecture has already been adequately discussed from both the experimental[3] and theoretical[3,6] points of view, in particular, by using the model to be here recalled.[6] In the second architecture (Fig. 1(d)), the FiM does not lie on a HM, and so interfacial asymmetric exchange vanishes. CDDWM is dominated by the spin transfer torques (STT), and DW precessional regimes emerge, due to reduced magnetostic interactions, resulting in DW velocities proportional to current magnitudes. Again, DW velocities have been found to maximize at T_A, when precession freezes, leading to a CDDWM characterized by rigid DWs, what is to be shown along this text.

II. TWO-SUBLATTICE MODEL OF FERRIMAGNETS

The description of the DW dynamics by means of a 1DM starts from the application of variational principles to the μM equation, i.e, the Landau-Lifshitz-Gilbert (LLG) equation.[9,10] This procedure is then augmented to study the magnetization dynamics in FiMs by posing two coupled LLG equations, that is, a two-sublattice model (TSLM). Details on the derivation of the 1DM equations for the TSLM are given in Ref. 6, so here we will only recall the required model parameters.

Within the model, the respective Gilbert constants of each sublattice are represented by the values α_i. The effective fields are the sum of the external field, the demagnetizing (magnetostatic) fields, the anisotropy fields, the isotropic exchange fields and the asymmetric exchange fields. The external field have components (B_x, B_y, B_z). The demagnetizing term possesses out-of-plane and in-plane components, given by the effective anisotropy constants $K_{eff,i}$ and $K_{sh,i}$. The asymmetric exchange provides a chiral character to some magnetic textures, whereas the isotropic one can be reduced on first approach to the sum of an intra-sublattice exchange field, given by the exchange stiffness A_i, and an inter-sublattice interaction due to the misalignment of both sublattices. The latter is accounted for by a parameter $B_{12} > 0$ (<0), which promotes the antiparallel (parallel) alignment of the sublattices. Finally, LLG equations also include the torques due to spin polarized currents, i.e., the STT[9] and the SOT.[10] Here, we focus our attention on the STT, consisting of adiabatic interactions and their non-adiabatic counterparts. The adiabatic interactions are defined by values u_i, proportional to the electric density current J_x flowing along the element, and calculated as $u_i = \frac{1}{2}\frac{g_i\mu_B P}{eM_{s,i}}J_x$, with μ_B being Bohr's magneton, e the electron charge, and P the degree of polarization of the spin current. The non-adiabatic interactions are proportional to the adiabatic ones by factors β_i.

The derivation of the 1DM requires the DW profile to be described in terms of the DW position q, width Δ and transition type Q. In the TSLM, the DW is considered to be composed of two transitions, one for each sublattice, which share the same q, and the same Δ (see Fig. 1(c) and (d)), but $Q_i = \pm 1$ establishes the transition type for each sublattice. $Q_i = +1(-1)$ means up-down (down-up) transition. Due to the antiferro coupling between sublattices, it follows that $Q_1 = -Q_2$.

## III. RESULTS AND DISCUSSION

When FiMs, such as GdFeCo or Mn$_4$N, are grown on top of certain substrates, the absence of interfacial asymmetric exchange[2,11] results in the formation of achiral DWs. The orientation of DW internal moments at rest is then dependent on purely geometrical aspects. In particular, for thin strips sufficiently wide, magnetostatic interactions determine the formation of Bloch-type walls. Importantly, due to the low net magnetization of FiMs as compared with ferromagnets, the magnetostatic interactions are rather low. If some parallelism between ferro- and ferrimagnets is made, Walker breakdown in FiMs is then expected to occur for rather low applied fields[12] or currents[13,14] in the temperature range around T_M. Consequently, the DW dynamics for moderate fields or currents is ruled by the precession of DW magnetic moments.

The case of the field-driven DW dynamics in ferrimagnetic GdFeCo alloys can be recalled at this point. This has been the subject of recent experimental work,[2] where fast field-driven antiferromagnetic spin dynamics is realized in FiMs at T_A. This behavior has been found to be reproducible with the TSLM. Our simulations have been carried out with a set of parameters similar to those considered in previous works,[3,6] but adapted as to take into account the absence of interfacial asymmetric exchange and SOTs. The parameters are: $A_i = 70\frac{pJ}{m}$, $K_{eff,i} \approx K_{u,i} = 1.4\frac{MJ}{m^3}$, $K_{u,i}$ being the magnetic uniaxial anisotropy constant of the FiM sublattices. With these parameters, DW width is $\Delta \approx 6nm$. Besides, $\alpha_i = 0.02$. Due to the low net magnetization in the temperature range of interest, $K_{sh,i} \approx 0$. The antiferromagnetic coupling is accounted for by the parameter $B_{12} = -9\frac{MJ}{m^3}$.[15] The gyromagnetic ratios ($\gamma_i = \frac{g_i\mu_B}{\hbar}$) are different due to distinct Landé factors: $g_1 = 2.2$ and $g_2 = 2.0$.[2] The Curie temperature is set to $T_C = 450K$, and $M_{s,1}^0 = 1.4\frac{MA}{m}$ and $M_{s,2}^0 = 1.71\frac{MA}{m}$, with $a_1 = 0.5$ and $a_2 = 0.76$. According to these values, $T_M \approx 241.5K$, and $T_A \approx 305K$. The dimensions of the FiM strips are $w \times t_{FiM} = 512nm \times 6nm$.

Fig. 2(a) presents the dependence of the DW terminal velocity, computed as $v_{st} = \frac{q(\Delta t) - q(0)}{\Delta t}$, with $\Delta t = 2ns$, on the out-of-plane applied field B_z at different temperatures. In agreement with

experiments,[2] v_{st} increase linearly with B_z, and the slope reaches a maximum at T_A. This fact is made clear in Fig. 2(b) where terminal velocity is represented as a function of temperature with B_z as a parameter. In all shown cases, no dynamics occurs at T_M since the net magnetization vanishes, whereas the highest speeds are found close to T_A. The clue for this behavior can be found in DW precession, represented as a function of temperature in Fig. 2(c). Precession frequencies are obtained as $\nu = \frac{\dot\psi_i(\Delta t)}{2\pi}$ ($i = 1, 2$), since $\dot\psi_1(\Delta t) \approx \dot\psi_2(\Delta t)$. The results demonstrate that DW magnetic moments precess during the dynamics, with a rather low misalignment, of a few minutes of arc, between the sublattices (not shown). Such a reduced misalignment is due to the strong interlattice interaction and seems to be irrelevant for the dynamics. Most importantly, precession freezes at temperatures around T_M and T_A, when the orientations of DW magnetic moments hold during the whole dynamics.

Previous field-driven analysis serves as a starting point to also understand the CDDWM in these elements, whose architecture promotes a dynamics purely governed by STT.[11] Fig. 2(d) and (g) present the dependence of the absolute terminal velocity as a function of the current J_x with the temperature as a parameter. The polarization has been set to $P = 0.7$, and the non-adiabatic transfer
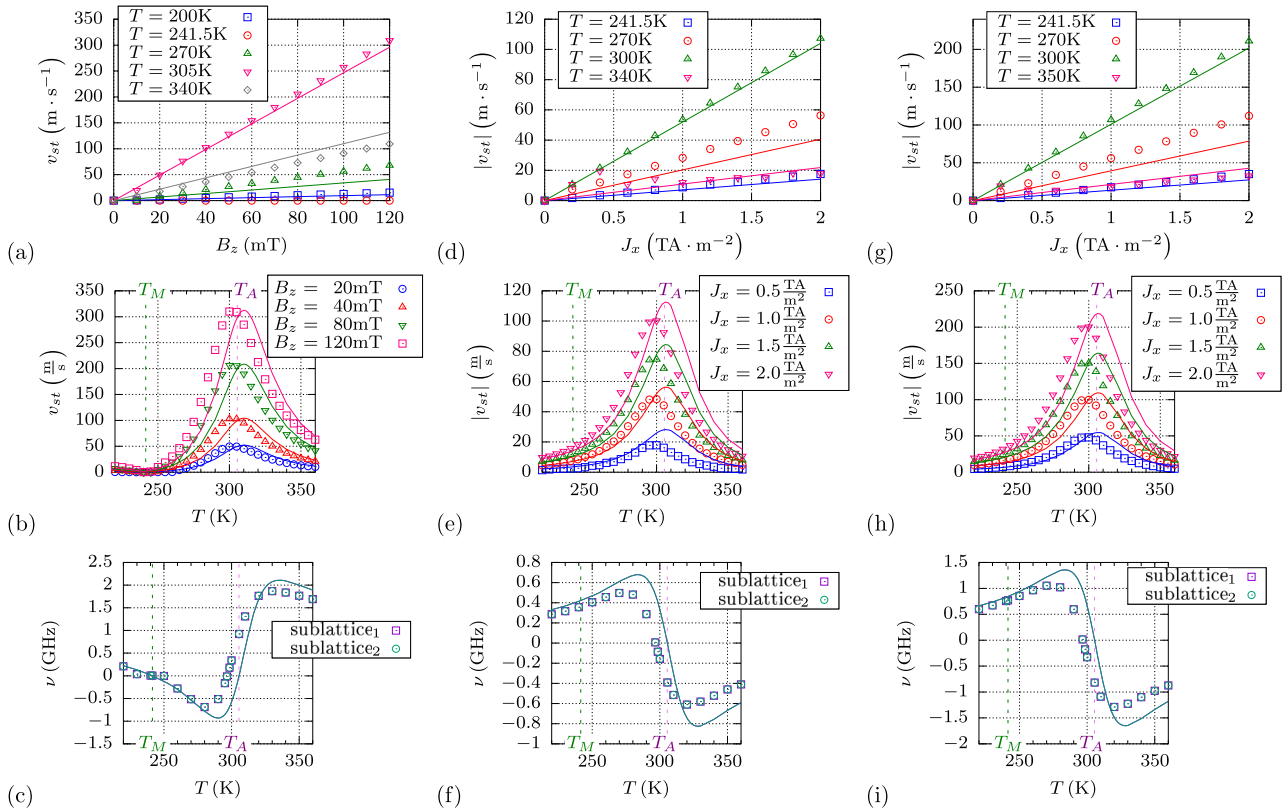
FIG. 2. Field-driven an current-driven dynamics in a FiM strip: (a) terminal velocity as a function of B_z with temperature as a parameter, (b) terminal velocity with B_z as a parameter and (c) precessional frequencies of DWs for $B_z = 40mT$ as functions of temperature, (d) and (g) terminal velocity as a function of J_x with temperature as a parameter, (e) and (h) terminal velocity with J_x as a parameter and (f) and (i) precessional frequency of DWs for $J_x = 1\frac{TA}{m^2}$ as functions of temperature. $\beta_i = \alpha_i$ for (d), (e) and (f), whereas $\beta_i = 2\alpha_i$ for (g), (h) and (i). Dots and continuous lines correspond respectively to full μM simulations and the 1DM results.
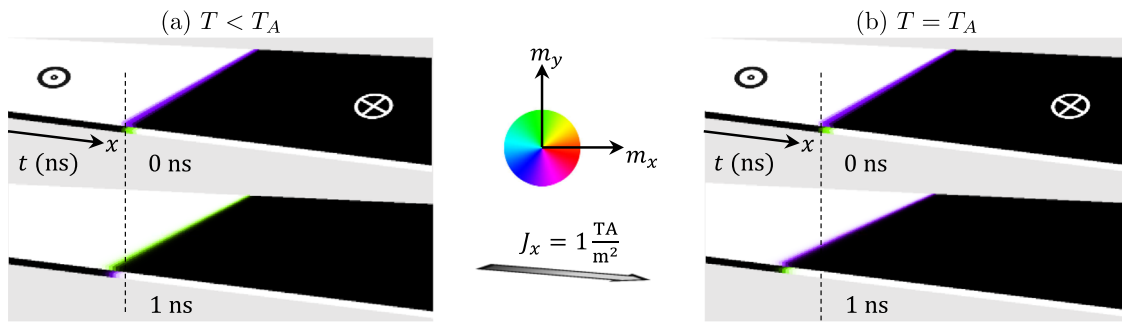
FIG. 3. Snapshots of the CDDWM in a FiM strip with $\beta_i = \alpha_i$ at (a) $T < T_A$, and (b) $T = T_A$.

torque parameters have been chosen as (d) $\beta_i = \alpha_i$ (also for figures (e) and (f)), and (g) $\beta_i = 2\alpha_i$ (also for figures (h) and (i)). Differently from the results obtained in the field-driven case, the CDDWM at T_M is not null, since the STT pushes the transitions in each sublattice in the same direction (and not in opposite directions as it occurs in the field-driven case). However, the maximum slope is again found at T_A, when the precessional frequency vanishes.

To show in more detail this behavior, Fig. 3 presents the snapshots of the CDDWM at two representative temperatures, for the case $\beta_i = \alpha_i$. The two sublattices composing the FiM are presented superposed, as to simplify the view, so one sublattice is on top of the other. The images in (a) correspond to the dynamics at $T < T_A$. In this case, the DW internal moments precess, and a turn of approximately 180° takes place within the 1ns-interval passing from the image on top to the bottom image. However, no precession takes place at $T = T_A$, as shown in (b). The distinct distances run by the DWs can be also compared.

Differently from the behavior of magnetic moments in pure ferromagnets, where STT compensates damping when $\beta_i = \alpha_i$, FiMs seem to present these precessing magnetic moments even in this case. Such precession would be associated with the torque due to the coupling between the two sublattices and freezes at T_A, a result that would not be in any case explainable by means of effective models.

IV. CONCLUSIONS

The aim of this work has been first to highlight the capacities of the TSLM and, particularly, the 1DM based on it, to reproduce recent experimental work on DW dynamics in FiMs. Differently from previous approaches, the TSLM does not require the use of effective parameters, but experimentally determined ones, which allows providing insightful details about the dynamics.

The work has been devoted to FiMs structured so that DWs adopt achiral Bloch configurations at rest, and the main conclusions of this work are as following. The DW dynamics in FiMs is characterized by DW precession, which freezes at T_A. Because of that, the DW velocity at T_A is enhanced, both for the field- and for the current-driven cases. Our results are also in good qualitative agreement with recent experimental observations: Ref. 2 for the field-driven case, and Ref. 11 for the current-driven one. Finally, the physical origin or the fundamental reasons behind these observations can only be achieved by adopting models which consider the independent but antiferromagnetically coupled nature

of the two sublattices forming the FiM. Therefore, our models will be useful to understand state-of-the-art experiments and also to develop and optimize future DW-based devices.

Final note: During the revision of the present manuscript we were aware of a recent work on field-driven and current-driven domain wall motion in single ferrimagnetic strips (Ref. 16). Our theoretical description is consistent with their experimental observations showing off a peak of field-driven DW terminal velocity at the angular compensation temperature T_A.

REFERENCES

[1]S. S. P. Parkin, M. Hayashi, and L. Thomas, "Magnetic domain wall racetrack memory," Science **320**, 190 (2008).

[2]K.-J. Kim, S. K. Kim, Y. Hirata, S.-H. Oh, T. Tono, D.-H. Kim, T. Okuno, W. S. Ham, S. Kim, G. Go, Y. Tserkovnyak, A. Tsukamoto, T. Moriyama, K.-J. Lee, and T. Ono, "Fast domain wall motion in the vicinity of the angular momentum compensation temperature of ferrimagnets," Nature Materials **16**, 1187–1192 (2017).

[3]L. Caretta, M. Mann, F. Büttner, K. Ueda, B. Pfau, C. M. Günther, P. Hessing, A. Churikova, C. Klose, M. Schneider, D. Engel, C. Marcus, D. Bono, K. Bagschik, S. Eisebitt, and G. S. D. Beach, "Fast current-driven domain walls and small skyrmions in a compensated ferrimagnet," Nature Nanotechnology **13**, 1154 (2018).

[4]S. A. Siddiqui, J. Han, J. T. Finley, C. A. Ross, and L. Liu, "Current-induced domain wall motion in a compensated ferrimagnet," Physical Review Letters **121**, 057701 (2018).

[5]Ó. Alejos, V. Raposo, L. Sanchez-Tejerina, R. Tomasello, G. Finocchio, and E. Martinez, "Current-driven domain wall dynamics in ferromagnetic layers synthetically exchange-coupled by a spacer: A micromagnetic study," Journal of Applied Physics **123**(1), 013901 (2018).

[6]E. Martínez, V. Raposo, and Ó. Alejos, "Current-driven domain wall dynamics in ferrimagnets: Micromagnetic approach and collective coordinates model," Journal of Magnetism and Magnetic Materials **491**, 165545 (2019).

[7]C. D. Stanciu, V. Kimel, F. Hansteen, A. Tsukamoto, A. Itoh, A. Kirilyuk, and T. Rasing, "Ultrafast spin dynamics across compensation points in ferrimagnetic GdFeCo: The role of angular momentum compensation," Physical Review B **73**, 220402(R) (2006).

[8]D.-H. Kim, T. Okuno, S. K. Kim, S.-H. Oh, T. Nishimura, Y. Hirata, Y. Futakawa, H. Yoshikawa, A. Tsukamoto, Y. Tserkovnyak, Y. Shiota, T. Moriyama, K.-J. Kim,

K.-J. Lee, and T. Ono, "Low magnetic damping of ferrimagnetic GdFeCo alloys," Physical Review Letters **122**, 127203 (2019).

[9]P. P. J. Haazen, E. Mure, J. H. Franken, R. Lavrijsen, H. J. M. Swagten, and B. Koopmans, Nature Materials **12**, 299 (2013).

[10]S. Zhang and Z. Li, Physical Review Letters **93**, 127204 (2004).

[11]T. Gushi, M. Jovičević Klug, J. Peña García, H. Okuno, J. Vogel, J. P. Attané, T. Suemasu, S. Pizzini, and L. Vila, "Mn$_4$N ferrimagnetic thin films for sustainable spintronics" (2019), arXiv:1901.06868 [cond-mat.mtrl-sci].

[12]A. Mougin, M. Cormier, J. P. Adam, P. J. Metaxas, and J. Ferré, "Domain wall mobility, stability and walker breakdown in magnetic nanowires," Europhysics Letters **5**, 57007 (2007).

[13]A. Thiaville, Y. Nakatani, J. Miltat, and N. Vernier, Journal of Applied Physics **95**(11), 7049 (2004).

[14]A. Thiaville, Y. Nakatani, J. Miltat, and Y. Suzuki, Europhysics Letters **69**, 990 (2005).

[15]C. T. Ma, X. Li, and S. J. Poon, "Micromagnetic simulation of ferrimagnetic TbFeCo films with exchange coupled nanophases," Journal of Magnetism and Magnetic Materials **417**, 197–202 (2016).

[16]T. Okuno, D.-H. Kim, S.-H. Oh, S. K. Kim, Y. Hirata, T. Nishimura, W. S. Ham, Y. Futakawa, H. Yoshikawa, A. Tsukamoto, Y. Tserkovnyak, Y. Shiota, T. Moriyama, K.-J. Kim, K.-J. Lee, and T. Ono, "Spin-transfer torques for domain wall motion in antiferromagnetically coupled ferrimagnets," Nature Electronics **2**, 389–393 (2019).